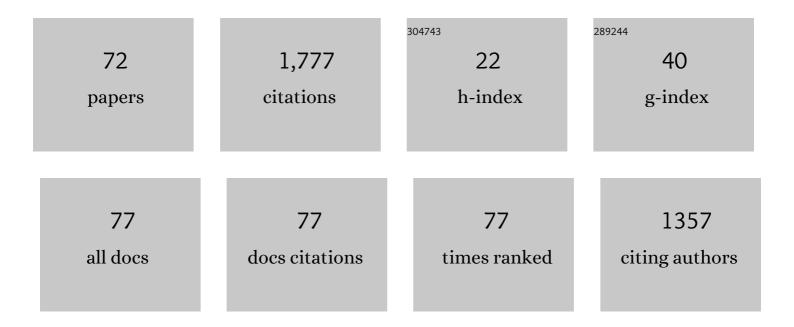


## List of Publications by Year in descending order

Source: https://exaly.com/author-pdf/914300/publications.pdf Version: 2024-02-01



CARV RUST

#	Article	IF	CITATIONS
1	Ionospheric Irregularity Layer Height and Thickness Estimation With a GNSS Receiver Array. IEEE Transactions on Geoscience and Remote Sensing, 2021, 59, 6198-6207.	6.3	2
2	Nightâ€Time Ionospheric Localized Enhancements (NILE) Observed in North America Following Geomagnetic Disturbances. Journal of Geophysical Research: Space Physics, 2021, 126, e2021JA029324.	2.4	6
3	Assimilation of GNSS Measurements for Estimation of High‣atitude Convection Processes. Space Weather, 2020, 18, e2019SW002409.	3.7	1
4	IDA4D: Ionospheric Data Assimilation for the ICON Mission. Space Science Reviews, 2020, 216, 1.	8.1	10
5	Tomographic Imaging of Traveling Ionospheric Disturbances Using GNSS and Geostationary Satellite Observations. Journal of Geophysical Research: Space Physics, 2020, 125, e2019JA027551.	2.4	7
6	Tomographic imaging of a large-scale travelling ionospheric disturbance during the Halloween storm of 2003. Annales Geophysicae, 2020, 38, 1149-1157.	1.6	0
7	Auroral Ionospheric Irregularity Properties via Estimation and Inverse Modeling of GNSS Scintillations. , 2019, , .		0
8	The Ionospheric Connection Explorer Mission: Mission Goals and Design. Space Science Reviews, 2018, 214, 1.	8.1	152
9	Intelligent systems for geosciences. Communications of the ACM, 2018, 62, 76-84.	4.5	71
10	Identifying E and F Region Irregularities with a Scintillation Auroral GPS Array. , 2018, , .		0
11	Identification of scintillation signatures on CPS signals originating from plasma structures detected with EISCAT incoherent scatter radar along the same line of sight. Journal of Geophysical Research: Space Physics, 2017, 122, 916-931.	2.4	28
12	Ionospheric data assimilation applied to HF geolocation in the presence of traveling ionospheric disturbances. Radio Science, 2017, 52, 829-840.	1.6	15
13	Distributed sensing of ionospheric irregularities with a GNSS receiver array. Radio Science, 2017, 52, 988-1003.	1.6	13
14	Inverse modeling of ionospheric irregularities observed using GPS scintillations at Poker Flat, AK. , 2017, , .		0
15	Assimilation of thermospheric measurements for ionosphereâ€ŧhermosphere state estimation. Radio Science, 2016, 51, 1818-1837.	1.6	6
16	Satelliteâ€beacon Ionosphericâ€scintillation Global Model of the upper Atmosphere (SIGMA) II: Inverse modeling with highâ€latitude observations to deduce irregularity physics. Journal of Geophysical Research: Space Physics, 2016, 121, 9188-9203.	2.4	26
17	Threeâ€dimensional modeling of highâ€latitude scintillation observations. Radio Science, 2016, 51, 1022-1029.	1.6	11
18	lonospheric data assimilation and forecasting during storms. Journal of Geophysical Research: Space Physics, 2016, 121, 764-778.	2.4	51

GARY BUST

#	Article	IF	CITATIONS
19	Modeled and observed equatorial thermospheric winds and temperatures. Journal of Geophysical Research: Space Physics, 2015, 120, 5832-5844.	2.4	11
20	First light from a kilometerâ€baseline Scintillation Auroral GPS Array. Geophysical Research Letters, 2015, 42, 3639-3646.	4.0	21
21	A novel data assimilation technique for the plasmasphere. Journal of Geophysical Research: Space Physics, 2015, 120, 8470-8485.	2.4	4
22	Community-wide model validation study for systematic assessment of ionosphere models. , 2015, , .		0
23	Ionospheric-thermospheric state estimation with neutral wind data assimilation. , 2015, , .		0
24	Properties of high latitude irregularities with a short-baseline 2D GPS scintillation array. , 2014, , .		0
25	Inferring 2D spatio-temporal properties of irregularities from a closely-spaced sub-auroral scintillation array. , 2014, , .		0
26	lonospheric irregularities during a substorm event: Observations of ULF pulsations and GPS scintillations. Journal of Atmospheric and Solar-Terrestrial Physics, 2014, 114, 1-8.	1.6	10
27	Effects of solar cycle 24 activity on WAAS navigation. Space Weather, 2014, 12, 46-63.	3.7	18
28	Satelliteâ€beacon Ionosphericâ€scintillation Global Model of the upper Atmosphere (SIGMA) I: Highâ€latitude sensitivity study of the model parameters. Journal of Geophysical Research: Space Physics, 2014, 119, 4026-4043.	2.4	40
29	GPS phase scintillation associated with optical auroral emissions: First statistical results from the geographic South Pole. Journal of Geophysical Research: Space Physics, 2013, 118, 2490-2502.	2.4	45
30	First stormâ€time plasma velocity estimates from highâ€resolution ionospheric data assimilation. Journal of Geophysical Research: Space Physics, 2013, 118, 7458-7471.	2.4	10
31	GEOScan: A global, real-time geoscience facility. , 2013, , .		8
32	An interhemispheric comparison of GPS phase scintillation with auroral emission observed at the South Pole and from the DMSP satellite. Annals of Geophysics, 2013, 56, .	1.0	10
33	GEOScan: a geoscience facility from space. Proceedings of SPIE, 2012, , .	0.8	2
34	Ionospheric scintillation over Antarctica during the storm of 5–6 April 2010. Journal of Geophysical Research, 2012, 117, .	3.3	45
35	Initial GPS scintillation results from CASES receiver at South Pole, Antarctica. Radio Science, 2012, 47, .	1.6	21
36	Global observations of <i>E</i> region plasma density morphology and variability. Journal of Geophysical Research, 2012, 117, .	3.3	8

GARY BUST

#	Article	IF	CITATIONS
37	Development and error analysis of nonlinear ionospheric removal algorithm for ionospheric electron density determination using broadband RF data. Journal of Geophysical Research, 2011, 116, n/a-n/a.	3.3	5
38	Deducing storm time <i>F</i> region ionospheric dynamics from 3-D time-varying imaging. Journal of Geophysical Research, 2011, 116, .	3.3	13
39	C/NOFS observations of intermediate and transitional scale-size equatorial spreadFirregularities. Geophysical Research Letters, 2009, 36, .	4.0	31
40	Estimating <i>E</i> region density profiles from radio occultation measurements assisted by IDA4D. Journal of Geophysical Research, 2009, 114, .	3.3	25
41	Neutral wind estimation from 4â€Ð ionospheric electron density images. Journal of Geophysical Research, 2009, 114, .	3.3	18
42	Mapping plasma structures in the high-latitude ionosphere using beacon satellite, incoherent scatter radar and ground-based magnetometer observations. Annals of Geophysics, 2009, 45, .	1.0	5
43	History, current state, and future directions of ionospheric imaging. Reviews of Geophysics, 2008, 46, .	23.0	210
44	Tracking of polar cap ionospheric patches using data assimilation. Journal of Geophysical Research, 2007, 112, n/a-n/a.	3.3	49
45	Observed and modeled thermosphere and ionosphere response to superstorms. Radio Science, 2007, 42,	1.6	30
46	Four-dimensional GPS imaging of space weather storms. Space Weather, 2007, 5, n/a-n/a.	3.7	53
47	Global thermosphere-ionosphere response to onset of 20 November 2003 magnetic storm. Journal of Geophysical Research, 2006, 111, .	3.3	105
48	Variations in the midlatitude and equatorial ionosphere during the October 2003 magnetic storm. Radio Science, 2006, 41, n/a-n/a.	1.6	9
49	Observations of the F region height redistribution in the storm-time ionosphere over Europe and the USA using GPS imaging. Geophysical Research Letters, 2006, 33, n/a-n/a.	4.0	19
50	Radio tomographic imaging of sporadic- <i>E</i> layers during SEEK-2. Annales Geophysicae, 2005, 23, 2357-2368.	1.6	22
51	Evidence for the tongue of ionization under northward interplanetary magnetic field conditions. Journal of Geophysical Research, 2005, 110, .	3.3	14
52	Radio tomographic imaging of the northern high-latitude ionosphere on a wide geographic scale. Radio Science, 2005, 40, n/a-n/a.	1.6	8
53	LOFAR as an ionospheric probe. Planetary and Space Science, 2004, 52, 1375-1380.	1.7	5
54	High-latitude plasma structure and scintillation. Radio Science, 2004, 39, n/a-n/a.	1.6	25

GARY BUST

#	Article	IF	CITATIONS
55	Ionospheric Data Assimilation Three-Dimensional (IDA3D): A global, multisensor, electron density specification algorithm. Journal of Geophysical Research, 2004, 109, .	3.3	180
56	Tomographic studies of aeronomic phenomena using radio and UV techniques. Journal of Atmospheric and Solar-Terrestrial Physics, 2002, 64, 1573-1580.	1.6	25
57	Verification of ionospheric sensors. Radio Science, 2001, 36, 1523-1529.	1.6	15
58	Computerized ionospheric tomography analysis of the Combined Ionospheric Campaign. Radio Science, 2001, 36, 1599-1605.	1.6	16
59	The Coherent Electromagnetic Radio Tomography (CERTO) experiment on ARGOS. , 2001, , .		1
60	IRI data ingestion and ionospheric tomography. Advances in Space Research, 2001, 27, 157-165.	2.6	22
61	Combined Ionospheric Campaign 1: Ionospheric tomography and GPS total electron count (TEC) depletions. Geophysical Research Letters, 2000, 27, 2849-2852.	4.0	43
62	Two-dimensional mapping of the plasma density in the upper atmosphere with computerized ionospheric tomography (CIT). Physics of Plasmas, 1998, 5, 2010-2021.	1.9	54
63	Ionospheric observations of the November 1993 storm. Journal of Geophysical Research, 1997, 102, 14293-14304.	3.3	21
64	Recent results of the CEDAR storm study. Advances in Space Research, 1997, 20, 1655-1664.	2.6	13
65	Mid-America Computerized Ionospheric Tomography Experiment (MACE '93). Radio Science, 1995, 30, 105-108.	1.6	17
66	Application of ionospheric tomography to single-site location range estimation. International Journal of Imaging Systems and Technology, 1994, 5, 160-168.	4.1	19
67	Were the Lyman-alpha clouds formed from shocks?. Astrophysical Journal, 1987, 319, 14.	4.5	7
68	Amplitudes and wavelengths of wavy Taylor vortices. Physics of Fluids, 1985, 28, 1243.	1.4	12
69	Mapping the Time-Varying Distribution of High-Altitude Plasma During Storms. Geophysical Monograph Series, 0, , 91-98.	0.1	5
70	Estimating Height and Thickness of an Ionospheric Irregularity Layer with a Closely-Spaced GNSS Receiver Array. , 0, , .		4
71	Auroral E and F Layer Ionospheric Irregularities Sensed by a Kilometer-Spaced GNSS Receiver Array. , 0, ,		1
72	A Night-time Ionospheric Localized Enhancement (NILE) During Extreme Storms. , 0, , .		0